AD-A152 251 THEORETICAL INVESTIGATION OF THREE-DIMENSIONAL SHOCK WAVE TURBULENT BOUND..(U) RUTGERS - THE STATE UNIV NEW BRUNSWICK N J DEPT OF MECHANICAL.. D D KNIGHT 1/1

UNCLASSIFIED 12 DEC 84 RU-TR-162-MIAE-F AFOSR-TR-85-0280 F/G 20/4 NL

END

FILMED

DTIC

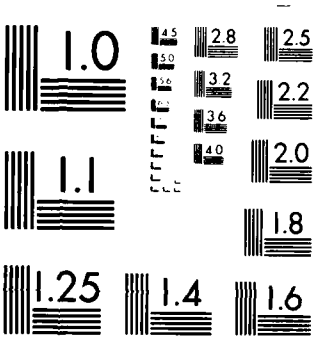

MICROCOPY RESOLUTION TEST CHART
NATIONAL BUREAU OF STANDARDS 1963-A

AFOSR-TR- 85-0280

(2)

THE STATE UNIVERSITY OF NEW JERSEY

Report RU-TR-162-MAE-F

THEORETICAL INVESTIGATION OF THREE-DIMENSIONAL SHOCK WAVE-TURBULENT BOUNDARY LAYER INTERACTIONS

Part III

Doyle D. Knight

DEPARTMENT OF MECHANICAL AND AEROSPACE ENGINEERING

Department of Mechanical and Aerospace Engineering
Rutgers University
New Brunswick, New Jersey 08903

Report RU-TR-162-MAE-F

THEORETICAL INVESTIGATION OF THREE-DIMENSIONAL SHOCK WAVE-TURBULENT BOUNDARY LAYER INTERACTIONS
Part III

Doyle D. Knight

Interim Report for Period 1 October 1983 to 30 September 1984
Approved for Public Release - Distribution Unlimited

Air Force Office of Scientific Research
Building 410
Bolling AFB
Washington, DC 20332

December 1984

UNCLASSIFIED

SECURITY CLASSIFICATION OF THIS PAGE *(When Data Entered)*

REPORT DOCUMENTATION PAGE		READ INSTRUCTIONS BEFORE COMPLETING FORM
1. REPORT NUMBER AFOSR-TR-	2. GOVT ACCESSION NO. AD-A152251	3. RECIPIENT'S CATALOG NUMBER
4. TITLE *(and Subtitle)* THEORETICAL INVESTIGATION OF THREE-DIMENSIONAL SHOCK WAVE-TURBULENT BOUNDARY LAYER INTERACTIONS - Part III		5. TYPE OF REPORT & PERIOD COVERED 1 Oct. 1983 - Annual 30 Sept. 1984 6. PERFORMING ORG. REPORT NUMBER
7. AUTHOR(s) Prof. Doyle D. Knight		8. CONTRACT OR GRANT NUMBER(s) AFOSR-82-0040
9. PERFORMING ORGANIZATION NAME AND ADDRESS Dept. of Mechanical and Aerospace Engineering, Rutgers University, New Brunswick, New Jersey 08903		10. PROGRAM ELEMENT, PROJECT, TASK AREA & WORK UNIT NUMBERS 61102F 2307/A1
11. CONTROLLING OFFICE NAME AND ADDRESS Air Force Office of Scientific Research/NA Building 410, Bolling AFB, DC 20332		12. REPORT DATE 12 December 1984 13. NUMBER OF PAGES 51
14. MONITORING AGENCY NAME & ADDRESS*(if different from Controlling Office)*		15. SECURITY CLASS. *(of this report)* UNCLASSIFIED 15a. DECLASSIFICATION DOWNGRADING SCHEDULE

16. DISTRIBUTION STATEMENT *(of this Report)*

Approved for Public Release; Distribution Unlimited

17. DISTRIBUTION STATEMENT *(of the abstract entered in Block 20, if different from Report)*

18. SUPPLEMENTARY NOTES

19. KEY WORDS *(Continue on reverse side if necessary and identify by block number)*

High Speed Flows; Viscous-Inviscid Interactions; Shock-Boundary Layer Interactions; Computational Fluid Dynamics; Navier-Stokes Equations; Turbulence

20. ABSTRACT *(Continue on reverse side if necessary and identify by block number)*

The focus of the research effort is the understanding of three-dimensional shock wave-turbulent boundary layer interactions. The approach uses the full mean compressible Navier-Stokes equations with turbulence incorporated through the algebraic turbulent eddy viscosity model of Baldwin and Lomax. The principal accomplishments of the third year may be categorized into four major areas. First, the Baldwin-Lomax model was evaluated for a series of non-separated two-dimensional turbulent boundary layers. Second, the 3-D Navier-Stokes codes was rewritten into CYBER 200 FORTRAN. Third, the computed results for the 3-D

DD FORM 1 JAN 73 1473 EDITION OF 1 NOV 65 IS OBSOLETE

UNCLASSIFIED

SECURITY CLASSIFICATION OF THIS PAGE *(When Data Entered)*

sharp fin α_g = 10 deg were compared with the results of a separate calculation by C. Horstmann using the k-ε turbulence model, and the experimental data of McClure and Dolling. Fourth, the 3-D sharp fin at α_g = 20 deg was computed, and the results compared with the available experimental data. The examination of the flowfield structure of the 3-D sharp fin at α_g = 20 deg was initiated.

PREFACE

This report presents the research accomplishments for the third year (1 October 1983 to 30 September 1984) of the research investigation entitled "Theoretical Investigation of Three-Dimensional Shock-Wave Turbulent Boundary Layer Interactions."

The research has benefited from the assistance of several individuals, including Dr. James Wilson (Air Force Office of Scientific Research), and Drs. James Keller and Jerry South (NASA Langley Research Center). The important and helpful interactions with S. Bogdonoff, S. Goodwin, C. Horstman and L. Smits are also acknowledged.

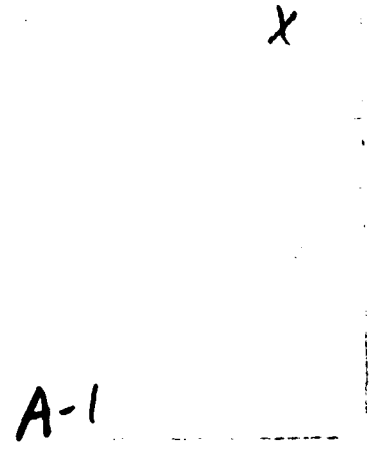

Table of Contents

List of Illustrations

List of Illustrations (cont'd)

List of Tables

Section I. Introduction

The overall goals of the theoretical research program, detailed in the original proposal (Knight 1981), remain the central focus of the research effort :

- To determine the accuracy of a theoretical model of 3-D shock wave-turbulent boundary layer interactions ("3-D turbulent interactions"), where the theoretical model consists of the 3-D mean compressible Navier-Stokes equations with a turbulent eddy viscosity

- To investigate the flow structure of 3-D turbulent interactions in simplified geometries through a close cooperative research effort between theory and experiment

- To evaluate the hypothesized physical structure of the 3-D turbulent interactions at a variety of conditions outside the range of experiments

These goals represent a chronological sequence of objectives. Clearly, the accuracy of theoretical predictions of 3-D turbulent interactions must be established by comparison with experiment prior to utilization of the computed results for the determination of the flowfield structure. A major portion of the first three years was devoted to this objective (Knight 1982, 1983) through a close collaboration with the Princeton Gas Dynamics Laboratory. The overall evaluations have been strongly favorable, and provide an impetus for achievement of the second goal. During the third year, the theoretical program has moved towards the second objective. In the following sections, the research accomplishments for the third year and research program for the fourth year are presented.

Section II. Research Accomplishments for the Third Year and Research Program for Fourth Year

A. Introduction

During the third year, significant progress was achieved towards the overall program objectives of determining the physical structure of 3-D turbulent interactions. The efforts can be categorized into several main areas :

1. Examination of Efficacy of Theoretical Model

A continued effort has been focused on the understanding of the accuracy of the theoretical model, in particular, the algebraic turbulent eddy viscosity of Baldwin and Lomax. In previous years (Knight 1982, 1983), the model was evaluated for 2-D turbulent interactions (the 2-D compression corner) and 3-D interactions (the 3-D sharp fin). During the third year, the effort on examination of the model focused on the following two major areas, namely 1) a series of 2-D turbulent boundary layers, and 2) the 3-D sharp fin. In the former case, discussed in Section II.B, the Baldwin-Lomax model was scrutinized for a variety of *unseparated adverse and favorable pressure gradient flows*. In the latter case, discussed in Section II.D, the computed results for the 3-D sharp fin at α_g = 10 deg (Knight 1984a, 1984b) were compared with recent computations by C. Horstman using the Jones-Launder (1972) two-equation k-ϵ turbulence model.

2. Further Development of Numerical Algorithm

The 3-D compressible Navier-Stokes code was rewritten into CYBER 200 FORTRAN during the third year. This effort is discussed in Section II.C.

3. Computation of 3-D Sharp Fin at α_g = 2Ø deg and Examination of Flow Structure

A series of computations were performed for the 3-D sharp fin at Mach 3 for α_g = 2Ø deg. The examination of the flowfield structure of the 3-D sharp fin at α_g = 2Ø deg was initiated. The computed results were employed to suggest the location for additional experimental investigations. This effort is discussed in Section II.E. Development of the numerical particle tracing program was initiated during the third year, with completion expected during the early part of the fourth year.

The research program for the fourth year is presented in Section II.F.

B. 2-D Turbulent Boundary Layer

An examination of the accuracy of the Baldwin-Lomax turbulence model (Baldwin and Lomax 1978) for two-dimensional turbulent boundary layers was completed during the third year (York 1984, York and Knight 1985). The objective of this research was to provide additional detailed fundamental information on the accuracy of the Baldwin-Lomax model for unseparated 2-D turbulent boundary layers in the presence of adverse and favorable pressure gradients and boundary layer bleed. This information was deemed critical to the success of the theoretical research program in 3-D turbulent interactions, wherein the turbulent boundary layers are subjected to regions of extended adverse/favorable pressure gradients. Despite the increasing popularity of the Baldwin-Lomax model, a detailed study of the behavior of the model for two-dimensional unseparated turbulent boundary layers had not been performed previously.

A compressible turbulent boundary layer code, developed under sponsorship of the Department of Mechanical and Aerospace

Engineering, Rutgers University, was utilized to compute the following cases (the references for the experimental data are indicated) :

1. Adiabatic Flat Plate Turbulent Boundary Layer (Mach numbers from 0 to 5) - Hopkins and Inouye 1971

2. Incompressible Turbulent Boundary Layer in Favorable, Zero, and Adverse Pressure Gradient - Schubauer and Klebanoff 1950

3. Incompressible Turbulent Boundary Layer in Zero Pressure Gradient with Uniform Bleed - Favre, Dumas, Verollet and Coantic 1966

4. Incompressible Turbulent Boundary Layer in Adverse Pressure Gradient with Uniform Bleed - Anderson, Kays and Moffat 1972

5. Supersonic Turbulent Boundary Layer in Adverse Pressure Gradient - Zwarts 1970

The first case provides a standard examination of the accuracy of the model for flat plate boundary layers. The second case has been used as a benchmark test for a number of turbulence models. Cases No. 3 to 5 were chosen by the 1980-81 AFOSR-HTTM-Stanford Conference on Complex Turbulent Flows (Kline et al 1981) as benchmark configurations.

The principal conclusions are the following :

- The constants C_{cp} and C_{Kleb} in the Baldwin-Lomax turbulence model depend weakly on the Mach number and Reynolds number of the flow. The values of these constants was determined by comparison with the Cebeci-Smith model (Cebeci and Smith 1974) over a range in

The initial condition for the computations was obtained by propogating the upstream flow profile (which matched the experimental upstream boundary layer) throughout the computational domain. The computed flowfield was judged converged to steady state after a physical time of approximately 3.5 t_c, where t_c is the time required for a fluid parcel to travel from the upstream to the downstream end of the mesh in the inviscid region. The computer time required was 2.Ø hrs on the VPS 32 for each computation. This represents an estimated factor of 14 to 2Ø times faster than a time-split vectorized version of MacCormack's explicit algorithm alone.

In Fig. 7, the computed and experimental surface pressure on the flat plate are displayed at three spanwise locations, specifically, z = 3.7 cm (2.92 δ_∞), 6.25 cm (4.92 δ_∞), and 8.79 cm (6.92 δ_∞). The computed results provide an accurate estimate of the upstream propogation of the interaction. Also, the plateau pressure is predicted with reasonable accuracy. In some of the regions of pressure gradient, however, the computed profiles do not agree closely with the experiment (e.g., Fig. 7c). This discrepancy may be due to the streamwise grid spacing ($\Delta x = \delta_\infty$). Although this was observed to be sufficient for the α_g = 1Ø deg case (Knight 1984b), wherein computations using streamwise grid spacing Δx = Ø.5 δ_∞ and 1.Ø δ_∞ were found to be essentially identical, the value $\Delta x = \delta_\infty$ may be insufficient for the present case.

A series of contour plots for several flow variables is presented in Figs. 8 to 11 at x/δ_∞ = 13. In Fig. 8, the static pressure is shown, with the location of the line of coalescence and the theoretical inviscid shock indicated by the letters "C" and "S", respectively. A broad region of constant pressure forms to the left (i.e., towards the sharp fin) of the line of coalescence, in agreement with previous computations. The pitot pressure contours (Fig. 9) display the characteristic "bulge" (Knight 1984a) associated with the overshoot in pitot pressure located

streamwise grid planes (N_x = 20) were employed which were uniformly spaced by an amount $\Delta x = \delta_\infty$. Within each plane, the mesh points were distributed in the y- and z-directions using a combination of geometric stretching near the flat plate and fin, and uniform spacing outside the boundary layers. The number of **ordinary** grid points in the y- and z-directions are N_y = 32 and N_z = 48. In addition, eight grid points (NSL = 8) were employed locally within the computational sublayer. A separate refined grid was utilized in the sublayer region in the immediate vicinity of the corner formed by the flat plate and the fin. A total of 40,140 grids points were utilized. The height of the first grid point adjacent to the fin or flat plate was less than 3.0 wall units at all locations (i.e., $\Delta y_2^+ \leq 3.0$, where $\Delta y_2^+ = \Delta y_2 u_* / \nu_w$, and Δy_2 is the distance of the first row of points from the flat plate ; a similar result holds for Δz_2, which is the distance of the first row of points adjacent to the fin). Two separate computations were performed in order to examine the sensitivity of the computed solution to the height z_m' of the computational sublayer adjacent to the flat plate. In each case, the maximum grid spacing in the y-direction $\Delta y_\infty = 0.58\delta_\infty$ and $0.59\delta_\infty$. The height of the computational domain in the y-direction is $8\delta_\infty$ for both cases. The width of the computational domain increases linearly from $13.0\delta_\infty$ at x = 0 to $28.6\delta_\infty$ at the furthest downstream plane. Likewise, the maximum grid spacing in the z-direction Δz_∞ varies from $0.42\delta_\infty$ to $1.07\delta_\infty$. The computed results using the two separate grids were found to be insensitive to the value of z_m' within the specified limits (Knight 1984b).

Table 4. Flow Conditions for Experiment of Goodwin (1984) and Computation for 3-D Sharp Fin at α_g = 20 deg

Case	δ_∞ (cm)	M_∞	$Re_{\delta\infty}$	$p_{t\infty}$ (kPa)	$T_{t\infty}$ (deg K)
Experiment	1.27	2.94	8.0×10^5	690	265
Computation	1.27	2.94	8.6×10^5	690	256

(16,60) and (24,60) deg, where α is the compression corner angle which is measured in the streamwise direction, and λ is the compression corner sweepback angle.

- To examine the flowfield structure of the 3-D sharp fin at higher fin angle α_g and compare with the structure at lower α_g

  The computation of the α_g = 20 deg case provides an entire family of 3-D sharp fin computations, ranging from α_g = 4 deg to 20 deg, which will be used to examine the effect of the shock strength on the flow structure.

- To collaborate with the experimental studies of the α_g = 20 deg sharp fin at the Princeton Gas Dynamics Laboratory

  The selection of the α_g = 20 deg case was significantly influenced by the existence of a concurrent experimental program at the Princeton Gas Dynamics Laboratory for the same configuration. The experimental study of the α_g = 20 deg sharp fin began with the work of Goodwin (1984) which includes measurement of surface pressure and oil film flow visualization. Based upon current schedules (Bogdonoff 1984), additional flowfield surveys including pitot pressure and yaw angle are planned in early 1985. **The concurrency of the theoretical and experimental programs provides an opportunity for an enhanced understanding of the flowfield structure.**

The flow conditions for the computation and experiment are indicated in Table 4. Two separate computations were performed for the α_g = 20 deg case. The numerical grid was generated according to the method of Knight (1984b). A total of 20

model provides a more accurate prediction for Case 1, while the Jones-Launder is more accurate in Case 2. Settles, Horstman and McKenzie (1984) observed that the Cebeci-Smith algebraic model overpredicted the surface yaw angle within the separated region of the 3-D swept compression corner, while the Jones-Launder model provided an accurate prediction. Second, the observed overshoot in yaw angle outside the boundary layer and upstream of the theoretical inviscid shock (Fig. 6a) is not predicted.

E. Computation of 3-D Sharp Fin at α_g = 20 deg

The principal focus of the research effort for the third year was the computation of the 3-D sharp fin at α_g = 20 deg at Mach 3. The objectives of this study are the following :

- To examine the accuracy of the Baldwin-Lomax model for stronger 3-D turbulent interactions

  The α_g = 20 deg case provides a more stringent examination of the capability of the theoretical model. The 3-D sharp fin interaction had previously been examined theoretically at values of $\alpha_g \leq$ 10 deg using the Baldwin-Lomax model (the theoretical inviscid pressure rise for α_g = 10 deg at Mach 3 is 2.1). The α_g = 20 deg case provides a stronger interaction (the theoretical inviscid pressure rise is 3.7), and thus a more critical examination of the model. In this regard, it is noted that in recent computations of the 3-D swept compression corner at Mach 3 by Horstman (Settles et al 1984, Horstman 1984a) using the two-equation k-ϵ model, a significant discrepancy was observed between the calculated and measured pressure distribution for two high sweepback angle cases (specifically, (α,λ) =

made by Settles, Horstman and McKenzie (1984) for a 3-D swept compression corner configuration for which separate computations were performed using the algebraic turbulent eddy viscosity model of Cebeci and Smith (1974) and the two-equation model of Jones and Launder (1972). The inner layer of the two-layer Cebeci-Smith model is essentially the same as the Baldwin-Lomax, while the outer layer formulations differ significantly.

- The computed pitot profiles are in generally good agreement with the experimental data. Similar agreement has been achieved by Knight (1984b) for the 3-D sharp fin data of Oskam et al (1976, 1977), and Settles, Horstman and McKenzie (1984) for the 3-D swept compression corner. A specific exception is the failure to accurately predict the overshoot in pitot pressure at $x_s/\delta_o = -1.47$ for Case 2.

- The computed yaw angle is sensitive to the turbulence model. Differences as large as 30% in the calculated surface yaw angle are observed, with the Baldwin-Lomax model typically yielding higher yaw angles near the surface. This is consistent with the results of Settles, Horstman and McKenzie (1984) concerning the Cebeci-Smith and Jones-Launder models for the 3-D swept compression corner.

- The computed yaw angle is in general agreement with experiment, although two specific deficiencies are noted. First, the computed profiles generally underpredict the measured yaw angle in the lower portion of the boundary layer. The Baldwin-Lomax model typically provides a more accurate prediction of the yaw angle in the immediate vicinity of the surface. Within the inner portion of the boundary layer, the Baldwin-Lomax

values of 34 deg and 24 deg using Baldwin-Lomax and Jones-Launder, respectively. In Fig. 5b (x_s/δ_o = 1.Ø), the author's computed profiles using Grid Nos. 1 and 2 are in close agreement. The author's profile is in close agreement with experiment, although underpredicting the experimental data for y/δ_∞ < Ø.4 . The profile of Horstman is in close agreement with experiment, except for y/δ_∞ < Ø.4, where it displays a more marked underprediction of yaw angle. The predicted surface yaw angles are 37 deg (Baldwin-Lomax) and 28 deg (Jones-Launder). Overall, the computed profiles of the author using Grid Nos. 1 and 2 are in excellent agreement. Furthermore, the predictions using the Baldwin-Lomax and Jones-Launder models are observed to be in good agreement with experiment with two exceptions. First, the measured overshoot in yaw angle (see Knight 1984c), occurring outside the boundary layer and upstream of the shock, is not predicted using either model. Second, both models typically underpredict the yaw angle within the lower part of the boundary layer, although the Baldwin-Lomax model yields a more accurate profile for this case.

In Fig. 6a, the computed and experimental yaw angle profiles for Case 2 are displayed at x_s/δ_o = -1.47 . The calculated profiles are again observed to underpredict the measured yaw angle near the wall, and fail to display the observed overshoot outside the boundary layer. At x_s/δ_o=3.4Ø (Fig. 6b), the computed profiles using the Jones-Launder model are in excellent agreement with experiment. The results using the Baldwin-Lomax model underpredict the observed profile. The predicted values of the yaw angle at the surface using both models are in good agreement with experiment.

In summary, the computations using the Baldwin-Lomax and the Jones-Launder models display the following major features :

- The computed pitot pressure is relatively insensitive to the turbulence model. A similar observation was

computed results of the author for the two grid systems (Nos. 1 and 2) are in excellent agreement. In addition, it is shown for Case 1 that the computed results for p_p using both the Baldwin-Lomax and Jones-Launder turbulence models are in good agreement with experiment.

In Fig. 4a, the calculated and measured p_p for Case 2 at $x_s/\delta_o = -1.47$ are displayed. Although achieving good agreement between theory and experiment within the boundary layer, both computations fail to accurately predict the peak pitot pressure outside the boundary layer, although the results of Horstman are seen to be in better agreement with the data. The reason for this discrepancy is not clear. In particular, it is noted that the relative grid spacing (in terms of the local flow conditions) for Case 2 for the author was smaller than the relative grid spacing for Case 1 as discussed previously. At $x_s/\delta_o = 3.40$ (Fig. 4b), the computed and measured profiles are seen to be in good agreement, with the exception of the region $y/\delta_\infty \leq 0.3$ where p_p is underestimated. Comparison of Figs. 3 and 4 indicate that the pitot pressure in this region is more accurately predicted for Case 1. Overall, it is concluded that the computed results for p_p for Case 2 using both the Baldwin-Lomax and Jones-Launder turbulence models are in general good agreement with experiment, with the exception cited above.

In Figs. 5 and 6, the computed results of the author and Horstman for the yaw angle are compared with the experimental data for Cases 1 and 2, respectively. In Fig. 5a, the computed results of the author for Case 1 at $x_s/\delta_o = -1.7$ using the two grid systems are again observed to be in excellent agreement. The author's profiles show generally good agreement with experiment, with a modest underestimate in the region $y/\delta_\infty < 0.4$. The profile of Horstman is in close agreement with the experiment for $y/\delta_\infty > 0.4$, although displaying a more significant underestimate of the yaw angle for $y/\delta_\infty < 0.4$. The predicted yaw angle at the surface differs markedly for the two turbulence models, with

and Dolling are indicated in Fig. 2. Profiles of the pitot pressure p_p and yaw angle (defined as the angle of the mean velocity vector in the plane of the flat plate) were measured at a series of streamwise locations at a fixed spanwise location z = 6.4 cm and 12.1 cm for Cases 1 and 2, respectively. The profiles were measured within the boundary layer on the flat plate, both upstream and downstream of the shock location. The number of experimental profiles each for p_p and yaw was 21 and 22 for Cases 1 and 2, respectively.

A selection of calculated and measured pitot pressure p_p profiles are shown in Figs. 3 and 4 for Cases 1 and 2, respectively, at locations upstream and downstream of the 3-D turbulent interaction. Additional profiles are provided in Knight (1984c). The locations of the profiles are indicated by x_s/δ_o, where $x_s = x-x_{shk}$, x_{shk} is the location of the theoretical inviscid shock wave at the particular spanwise location z, and δ_o is the boundary layer thickness on the flat plate at $(x,z) = (x_{shk},z)$ in the absence of the fin. The shock location x_{shk} is z = 12.Ø cm and 22.8 cm for Cases 1 and 2, respectively. The local undisturbed boundary layer thickness δ_o is Ø.59 cm and 1.55 cm, respectively.

In Fig. 3a, the computed p_p profiles of the author for Case 1 at $x_s/\delta_o = -1.7$ using the two different grid systems (Grid Nos. 1 and 2) are seen to been in excellent agreement. The comparison between the author's profiles and the experimental data is good, with the computations accurately predicting the peak value of the "overshoot" in p_p located outside the boundary layer. Within the boundary layer, the author's computations show good agreement with the measurements except for $y/\delta\infty < Ø.5$ where the pitot pressure is modestly overestimated. The p_p profile of Horstman is observed to be in good agreement with experiment, accurately predict the peak value of the "overshoot" in pitot pressure. At $x_s/\delta_o = 1.Ø$ (Fig. 3b), the results of both computations are in close agreement with experiment. Overall, it is evident that the

Table 3. Flow Conditions for Calculations of Horstman (1984b) for 3-D Sharp Fin for α_g = 10 deg

Case No.	δ_∞ (cm)	M_∞	$Re_{\delta\infty}$	$p_{t\infty}$ (kPa)	$T_{t\infty}$ (deg K)
1	0.54	2.94	3.41×10^5	690	267
2	1.4	2.94	8.83×10^5	690	267

The numerical grids employed by the author for Cases 1 and 2 are detailed in Knight (1984a, 1984b). For Case 1, two separate grid systems (denoted Grid Nos. 1 and 2) were employed. These grids differed principally in the height z'_m of the computational sublayer adjacent to the flat plate. The purpose of performing these two separate computations was to investigate the sensitivity of the calculated solution to the height of the computational (see Knight 1984a).

The numerical grids utilized by Horstman (1984b) for Cases 1 and 2 employed a uniform streamwise spacing $\Delta x = 1.1\delta_\infty$ and $0.39\delta_\infty$, respectively. This is comparable to the values $\Delta x = 1.1\delta_\infty$ and $0.49\delta_\infty$ for Knight (1984a). The grid spacing in the y- and z-directions was stretched exponentially near the surface and followed by uniform spacing. The uniform spacing Δy_∞ in the y-direction was $1.1\delta_\infty$ and $0.39\delta_\infty$ for Case 1 and 2, respectively. The corresponding grid spacing for the author is $0.68\delta_\infty$ and $0.62\delta_\infty$, respectively. The uniform spacing Δz_∞ in the z-direction was equal to Δy_∞ for Horstman. The corresponding grid spacing for the author was $0.29\delta_\infty$ to $1.2\delta_\infty$ for Case 1, and $0.53\delta_\infty$ for Case 2. A total of 90,112 grid points each were used by Horstman for Cases 1 and 2. The author employed 106,316 points for Case 1 and 79,727 points for Case 2.

The location of the boundary layer measurements of McClure

tations of Knight (1984a, 1984b) solve the 3-D Navier-Stokes equations using a hybrid explicit-implicit method (Knight 1984b), with turbulence incorporated using the algebraic eddy viscosity model of Baldwin and Lomax.

The flow conditions for the computations are presented in Tables 2 and 3. It is noted that there is a slight difference in Reynolds number for Case 2 between the author and McClure and Dolling. This is due to the fact that the freestream conditions for the author's computation were chosen to closely match the experimental test conditions of Oskam et al (1976, 1977). For the computations by the author, the flat plate surface temperature was 280.6 deg K, and the fin surface temperature was 280.6 and 252.8 deg K, respectively, for Cases 1 and 2. These values were chosen on the basis of the experimental conditions, and are close to adiabatic conditions. For the computations by Horstman, the flat plate and fin surfaces were assumed adiabatic.

Table 2. Flow Conditions for Calculations of Knight (1984a,b) for 3-D Sharp Fin for α_g = 10 deg

Case No.	δ_∞ (cm)	M_∞	$Re_{\delta\infty}$	$p_{t\infty}$ (kPA)	$T_{t\infty}$ (deg K)
1	0.45	2.91	2.75×10^5	690	276
2	1.37	2.94	9.25×10^5	690	256

- To determine the sensitivity of various flow variables to the turbulence model
- To seek a unifying understanding of any defects in the models

In the Spring of 1984, Dr. C. C. Horstman (NASA Ames Research Center) initiated a series of computations for the 3-D sharp fin (Fig. 1) at α_g = 1Ø deg and Mach 3 for two different Reynolds numbers. The specific flow conditions were chosen to correspond to the experimental conditions of McClure and Dolling (1983) (see also McClure 1983) which are indicated in Table 1, where $p_{t\infty}$ and $T_{t\infty}$ are the upstream total pressure and total temperature, respectively. A similar set of computations had been previously performed by the author (Knight 1984a, 1984b) and compared with the data of McClure and Dolling. Consequently, the opportunity arose for comparison of the results obtained from the two different turbulence models.

Table 1. Flow Conditions for Experiments of McClure and Dolling (1983) for 3-D Sharp Fin for α_g = 1Ø deg

Case No.	δ_∞ (cm)	M_∞	$Re_{\delta\infty}$	$p_{t\infty}$ (kPa)	$T_{t\infty}$ (deg K)
1	Ø.45	2.91	$2.75 \times 1Ø^5$	69Ø	276
2	1.29	2.93	$8.Ø \times 1Ø^5$	69Ø	271

The calculations of Horstman (1984b) solve the mean compressible 3-D Navier-Stokes equations using the explicit-implicit algorithm of MacCormack (1982), with the effects of turbulence incorporated using the two-equation k-ϵ model of Jones and Launder (1972) together with the wall function boundary conditions of Viegas and Rubesin (1983) (see also Horstman 1984a). The compu-

the use of the 32-bit word length (only 64-bit word was supported). The SL/1 language was chosen for two reasons, namely 1) the computing time required using the 32-bit word is half as much as required by the 64-bit word, and 2) the storage requirement using the 32-bit word is half as much as the 64-bit word.

NASA Langley terminated support of the SL/1 language in September 1984, due to the upgrade of their supercomputer facility from a CYBER 203 to a VPS 32, and the conversion of the Operating System from OS Version 1.4 to VSOS Version 2.1. This latter version of the Operating System is not compatible with SL/1. It is noted that SL/1 was available only at NASA Langley.

Consequently, a significant effort was expended during the first nine months of the third year in rewriting the 3-D Navier-Stokes code and an auxiliary 3-D coordinate generation code into CDC CYBER 200 FORTRAN Version 2 (this later version of CDC CYBER FORTRAN does provide support of the 32-bit word length). The rewriting effort and test computations were completed in June 1984, and the code was employed in the computation of the 3-D sharp fin at α_g = 20 deg (see Section II.E).

D. Comparison of 3-D Sharp Fin Results at α_g = 10 deg Using the Baldwin-Lomax and Jones-Launder Turbulence Models

An important element of the research effort in 3-D interactions is the understanding of the significance of the specific turbulence model for the prediction of the flowfield. Several objectives can be identified, including :

- To assess the relative accuracy of the Baldwin-Lomax algebraic model compared to other models (e.g., the two-equation k-ε model)

81 AFOSR-HTTM-Stanford Conference on Complex Turbulent Flows.

- The calculated results for c_f, δ^*, θ and velocity profile for the adverse-pressure-gradient/uniform bleed incompressible boundary layer of Anderson et al (1972) are in good agreement with the experimental data. In comparison with the results of other turbulence models used in the 1980-81 AFOSR-HTTM-Stanford Conference on Complex Turbulent Flows, the Baldwin-Lomax model was amongst the group which was in closest agreement with experiment.

- For the supersonic adverse-pressure-gradient case of Zwarts (1970), the calculated results for c_f, shape factor H and velocity profiles are in close agreement with the experimental data. In comparison with four other turbulence models used in the 1980-1981 AFOSR-HTTM-Stanford Conference, the results obtained using the Baldwin-Lomax model for c_f and H were amongst those in closest agreement with the experiment. The computed momentum thickness development, however, underpredicts the experimental data, with a maximum discrepancy less than 30%. A similar discrepancy was observed in the other models examined in the Conference.

C. Rewriting 3-D Navier-Stokes Code into CDC CYBER FORTRAN

The 3-D Navier-Stokes code was originally written during 1980 to 1982 in the SL/1 computing language developed by John Knight (1979) at NASA Langley Research Center. The SL/1 language was a powerful, vector-processing language which provided the capability for 32-bit word computation. At that time the only other available language on the CYBER 203 was Control Data Corporation's (CDC) CYBER FORTRAN Version 1.4, which did not permit

Mach number from zero to five. This evaluation extends the original investigation of Baldwin and Lomax (1978), who evaluated C_{cp} and C_{Kleb} by comparison with the Cebeci-Smith model at transonic speeds only, and the earlier investigations of the values for C_{cp} and C_{Kleb} by Visbal (1983) and Knight (1984b) at Mach zero and Mach 3, respectively.

The computed results for skin friction coefficient c_f using the revised values of C_{cp} and C_{Kleb} were compared with the Van Driest II Theory using the Karman-Schoenherr equation. According to Hopkins and Inouye (1971), the Van Driest II theory provides the best correlation of experimental data for skin friction on adiabatic flat plates. The computed results are observed to yield a modest improvement compared to the results obtained using the original model constants.

- Excellent agreement is obtained with the experimental data of Schubauer and Klebanoff for the favorable/-zero/adverse pressure-gradient incompressible boundary layer at all stations upstream of separation. The data included skin friction coefficient c_f, displacement thickness δ^*, momentum thickness θ and velocity profiles. The computed results are in close agreement with previous computations using the Cebeci-Smith model.

- The computed velocity profiles for the uniform bleed incompressible boundary layer of Favre et al (1966) are in close agreement with experiment. Detailed comparison of Reynolds stress profiles shows reasonable agreement with experiment, with the discrepancy decreasing with increasing bleed. The computed Reynolds stress profiles are comparable to the results obtained by a number of other turbulence models employed in the 1980-

outside the boundary layer and immediately upstream of the shock. The "bulge" coincides with the compression region that forms upstream of the shock wave (Oskam et al 1976). The pitch angle, defined by $\tan^{-1}(v/(u^2+w^2)^{1/2})$ where (u,v,w) are the velocity components in the (x,y,z) coordinates, is shown in Fig. 10. Regions of positive and negative pitch develop, associated with the shock boundary layer interaction and corner region, respectively, in agreement with the results at lower α_g. The largest pitch angle is observed to occur outside the boundary layer and to the left of the line of coalescence. The yaw angle, defined by $\tan^{-1}(w/u)$, is displayed in Fig. 11. A region of large yaw angle develops adjacent to the surface. Also, the yaw angle is less than the fin angle in a region above the boundary layer on the flat plate and between the sharp fin and the shock. This region corresponds to fluid moving towards the fin. Both of these observations are consistent with previous results at lower values of α_g. In Fig. 12, the surface streamlines are illustrated. The distinct line of coalescence is clearly indicated.

A detailed analysis of the α_g = 20 deg flowfield is in progress, in combination with the development of the numerical particle-tracing algorithm and comparison with the proposed experimental data (Section II.F).

F. Research Program for Fourth Year

The principal focus of research for the fourth year is the investigation of the physical structure of 3-D turbulent interactions for simplified geometries. This represents the continued evolution of the theoretical research effort towards greater understanding of physical flowfield stucture. This evolution has been possible due to the success of the theoretical model. **It must be emphasized, however, that a continued examination of the efficacy of the model under different flow conditions (through comparison with experimental data) is**

essential to insure the fidelity of the flowfield structures deduced from the theoretical results.

The theoretical research is intended to be closely coupled to the experimental research effort at the Princeton Gas Laboratory. The principal modes of interaction of the theoretical and experimental efforts include the following :

- o Computation of selected 3-D interaction flows prior to experiment to assist in the determination of the location for flowfield measurements

- o Evaluation of the flowfield structure of 3-D interactions using the computed and experimental results, development of flow structure models, and design of new experiments to evaluate the flow models

Three major tasks have been identified for the remainder of the fourth year, and are discussed below.

Task No. 1 : Comparison with Proposed Experimental Data for 3-D Sharp Fin at α_g = 2Ø

The computed flowfield solution for the 3-D sharp fin at α_g = 2Ø deg, obtained during the third year (Section II.E), will be compared with additional experimental data scheduled for acquisition in 1985 at the Princeton Gas Dynamics Laboratory (Bogdonoff 1984). This data includes boundary layer profiles of pitot pressure and yaw angle.

The experimental and theoretical investigations of the 3-D sharp fin at α_g = 2Ø deg represent a significant example of collaboration between Rutgers University and the Princeton Gas Dynamics Laboratory. The computed flowfield has provided an indication of suitable locations for experimental boundary layer measurements (see Section III.B.7). The experimental data will

provide the opportunity for further examination of the efficacy of the theoretical model. Together, the theoretical and experimental results will provide new insight into the structure of the 3-D sharp fin interaction.

Task No. 2 : Physical Structure of 3-D Sharp Fin Flowfield

The structure of the 3-D supersonic sharp fin flowfield, and its dependence on the strength of the interaction (i.e., fin angle α_g and Mach number M_∞), remain important questions. Token (1974) proposed a vortex-dominated flowfield model to account for the high heat transfer rates observed near the intersection of the sharp fin and flat plate (tunnel wall). Korkegi (1976) proposed a vortex model associated with flow separation on the flat plate, with the appearance of a secondary vortex for stronger interactions. Oskam et al (1976, 1977) criticized Korkegi's model on the basis of their experimental data, which indicated the absence of "separation". Kubota and Stollery (1982) criticized the single vortex model of Token, and proposed a double-vortex model. Zheltovodov (1982) extended the model of Korkegi to include a total of six fundamental interaction regimes including the disappearance and subsequent reappearance of secondary separation for stronger interactions.

The objective of this research effort is to investigate the structure of the previously computed 3-D sharp fin flowfields at Mach 3. This numerical data base covers a range of Reynolds numbers $Re_\delta = 2.8 \times 10^5$ to 9.3×10^5 and fin angles $\alpha_g = 4$ deg to 20 deg. A combination of numerical particle tracing, surface flow graphics (i.e., limiting streamlines, which are related to experimental surface oil flow pictures) and flowfield contour plots will be employed. This combined approach is necessary to provide an understanding of the relationship between the flow structure and its surface representation (i.e., limiting streamlines), since there is no unique relationship between the pattern

of wall streamlines and the flowfield above the wall (Dallman 1983).

Task No. 3 : Computation of 3-D Swept Compression Corner

The three-dimensional swept compression corner, described in terms of the compression corner angle α (measured in the streamwise direction) and sweepback angle λ (Fig. 13), represents an important family of 3-D turbulent interactions. The 3-D sharp fin and 2-D compression ramp may be considered specific cases of the 3-D swept compression corner family corresponding to (α,λ) equal to $(90,\alpha_g)$ and $(\alpha,0)$ deg, respectively. Extensive experimental data has been obtained for a large number of configurations of the 3-D swept compression corner at Mach 3 at the Princeton Gas Dynamics Laboratory (Settles et al 1980, Settles et al 1982, Mc Kenzie 1983, Settles and Teng 1984). The data includes surface pressure and kerosene-lampblack surface flow visualization for more than forty different (α,λ) configurations at values of α and λ up to 24 deg and 70 deg, respectively. Detailed flowfield surveys of pitot pressure and yaw angle have been obtained for (α,λ) = (24,40) deg at two different Reynolds numbers.

Horstman has calculated a series of 3-D swept compression corner configurations using the 3-D mean compressible Navier-Stokes equations (Settles et al 1984, Horstman 1984a). The (α,λ) = (24,40) deg configuration was computed at two Reynolds numbers using the algebraic eddy viscosity model of Cebeci-Smith (1974) and the two-equation $k - \epsilon$ model of Jones-Launder (1972). The computed results were found to be in reasonable agreement with experiment, although discrepancies were noted in the surface pressure distribution. In addition, a total of thirty-five (35) different configurations were calculated at various (α,λ) using the $k - \epsilon$ model. The numerical results displayed close agreement with the measured boundary in the (α,λ) plane between cylindrical

and conical flow. Good agreement was obtained with experimental data for surface pressure for a number of (α,λ) configurations. The model, however, failed to accurately predict the surface pressure distribution for high sweepback angles (e.g., (a, λ) = (24, 60)), for which the flow exhibited a large separation region inferred from the surface streamlines. Horstman was unable, however, to conclude whether this disagreement was attributable to a deficiency in the $k - \epsilon$ model or insufficient grid resolution (Horstman 1984a). Recently, Horstman (1984b) recomputed the (α, λ) = (24, 60) case using a refined grid. The calculated surface pressure, however, was found to be in significant disagreement with experiment.

A series of 3-D swept compression corner configurations at Mach 3 will be computed using the Baldwin-Lomax model. The choice of each configuration (e.g., α, λ and Reynolds number Re_δ) will based upon existing experimental data and planned experimental investigations at the Princeton Gas Dynamics Laboratory. The objectives of this research effort are the following :

- To examine the accuracy of the Baldwin-Lomax model for the class of 3-D swept compression corner interactions

  The extensive experimental data, including surface measurements (pressure distribution and kerosene-lamp-black surface streamline visualization) and flowfield surveys (pitot pressure and yaw angle profiles for (α,λ) = (24,40) deg), provide an opportunity for continued examination of the efficacy of the Baldwin-Lomax model. In this regard, it is noted that additional grid-resolution studies for the 3-D swept compression corner may be required (similar to the study performed for the 3-D sharp fin (Knight 1984a,b)) in order to yield definitive conclusions concerning the accuracy of the Baldwin-Lomax model for this class of 3-D interactions.

- To examine the sensitivity of the computed flowfield to the turbulence model employed

  The proposed computations using the Baldwin-Lomax model, combined with the previous results by Horstman (Settles et al 1984), provide the opportunity for additional examination of the sensitivity of the computed flow to the turbulence model employed.

- To provide a theoretical data base for detailed analysis of the flowfield structure

  A careful flowfield analysis is planned during the following year utilizing the computed results.

Section III. Publications and Scientific Interactions

Period : 1 October 1983 to 30 September 1984

A. Written Publications

1. Knight, D., "Numerical Simulation of Three-Dimensional Shock-Turbulent Boundary Layer Interaction Generated by a Sharp Fin", AIAA Paper No. 84-1559, AIAA 17th Fluid Dynamics, Plasmadynamics and Lasers Conference, June 25-27, 1984 (submitted to AIAA J.) [**]

2. Visbal, M., and Knight, D., "Evaluation of the Baldwin-Lomax Turbulence Model for Two-Dimensional Shock Wave Boundary Layer Interactions", AIAA J., Vol. 22, July 1984, pp. 921-928 (AIAA Paper No. 83-1697, 1983) [**]

3. Knight, D., "A Hybrid Explicit-Implicit Numerical Algorithm for the Three-Dimensional Compressible Navier-Stokes Equations", AIAA J., Vol. 22, Aug 1984, pp. 1056-1063 (AIAA Paper No. 83-0223, 1983) [*] [**]

[*] Research sponsored by AFOSR Grant 80-0072
[**] Research sponsored by AFOSR Grant 82-0040

B. Interactions with Research Group at Princeton Gas Dynamics Laboratory

1. 25 October 1983 : Meeting with Princeton Gas Dynamics Lab Research Group

   Topics : 1) Discussion of recent experimental work at Princeton on 3-D swept compression corner at Mach 2, and 3-D sharp fin at Mach 3 at higher fin angles.

   2) Discussion of recent theoretical work on 3-D sharp fin at Mach 3 and $Re_{\delta} = 2.8 \times 10^5$, and examination of contour maps for pitot pressure and pitch angle.

   3) Discussion of theoretical research program for current year.

   4) Discussion of theoretical and experimental research objectives for future years.

2. 14 February 1984 : Meeting with S. Bogdonoff

   Topics : 1) Discussion of theoretical and experimental research objectives for future years.

   2) Discussion of flow structure of 3-D swept compression corner at high sweep angles.

3. 20 April 1984 and 4 May 1984: Conversation with S. Bogdonoff

   Topics : 1) Discussion of immediate experimental research program for 3-D sharp fin at high fin angles.

   2) Discussion of theoretical research program for remainder of current year.

4. 4 May 1984 : Conversation with S. Bogdonoff

   Topics : 1) Discussion of upstream flow conditions for computation of 3-D sharp fin at $\alpha_g = 20$ deg

5. 5 July 1984 : Conversation with S. Bogdonoff

Topics : 1) Discussion of experimental configuration and available data for 3-D sharp fin at α_g = 20 deg.

6. 7 August 1984 : Conversation with S. Bogdonoff

Topics : 1) Discussion of collaborative exchange using computed results for 3-D sharp fin at α_g = 20 deg to assist in choosing locations for proposed experimental boundary layer measurements

2) Discussion of future experimental and computational work

7. 30 August 1984 : Meeting with Princeton Gas Dynamics Lab Research Group

Topics : 1) Presentation of computed results for 3-D sharp fin at α_g = 20 and comparison with experimental data of Scott Goodwin (Princeton Gas Dynamics Lab) for surface pressure and surface streamlines. Discussion of flow structure for 3-D sharp fin.

2) Discussion of possible locations for planned experimental boundary layer measurements for 3-D sharp fin at α_g = 20 deg.

3) Discussion of experimental results of Goodwin concerning secondary lines of coalescence.

C. Interactions with NASA Ames Research Center

1. 9 February and 17 April 1984 : Conversation with C. Horstman
   Topic : 1) Discussion of recent computations at NASA Ames on swept compression corner at Mach 3.
   2) Discussion of recent computations at Rutgers on 3-D sharp fin at Mach 3.

2. 20 July 1984 : Conversation with C. Horstman
   Topic : 1) Discussion of recent computations at NASA Ames on 3-D sharp fin for $Re_\delta = 9 \times 10^5$ and comparison with previous computation by Knight.

3. 6 August 1984 : Conversation with C. Horstman
   Topic : 1) Discussion of recent computatinos at NASA Ames on 3-D sharp fin for $Re_\delta = 2.8 \times 10^5$ and comparison with previous computation by Knight.

D. Spoken Papers Presented at Technical Meetings

1. Knight, D., "Computation of Three-Dimensional Viscous Flow in a Supersonic Diffuser", Thirty-Sixth Annual Meeting, Division of Fluid Dynamics, American Physical Society, 20-22 November 1983, Bulletin of the American Physical Society, Vol. 28, No. 9, November 1983, p. 1394.

E. Seminars - October 1983 to Present

1. Knight, D., "Numerical Simulation of 3-D Shock-Turbulent Boundary Layer Interactions", Dept. of Aerospace Engineering, Syracuse University, March 1984.

Section IV. List of Personnel and Degrees Awarded

A. Personnel

Principal Investigator : Prof. Doyle Knight
Dept. of Mechanical and
Aerospace Engineering

Graduate Research Assistant : Mr. Brian York
Dept. of Mechanical and
Aerospace Engineering

Mr. Cho Ong
Dept. of Mechanical and
Aerospace Engineering

B. Degrees Awarded

Brian York
M.S., Mechanical and Aerospace Engineering, October 1984
Thesis title : "Evaluation of the Baldwin-Lomax Turbulence
Model for a Class of Boundary Layer Flows"
Thesis Advisor : Prof. Doyle Knight

Section V. References

Anderson, P., Kays, W., and Moffat, R. 1972 The Turbulent Boundary Layer on a Porous Plate : An Experimental Study of the Fluid Mechanics for Adverse Free-Stream Pressure Gradients. Thermosciences Division, Dept. Mechanical Engineering, Stanford U., Report No. HMT-15.

Baldwin, B., and Lomax, H. 1978 Thin Layer Approximation and Algebraic Model for Separated Turbulent Flows. AIAA Paper No. 78-257.

Bogdonoff, S. 1984 Private Communication : December 1984.

Cebeci, T., and Smith, A. 1974 Analysis of Turbulent Boundary Layers. Academic Press.

Dallmann, U. 1983 Topological Structures of Three-Dimensional Vortex Flow Separation. AIAA Paper No. 83-1735.

Favre, A., Dumas, R., Verollet, E., and Coantic, M. 1966 Couche Limite Turbulente sur Paroi Poreuse avec Aspiration. J. de Mechanique, 5, pp. 3-28.

Goodwin, S. 1984 An Exploratory Investigation of Sharp-Fin Induced Shock Wave/Turbulent Boundary Layer Interactions at High Shock Strengths. MS Thesis, Dept. Aero. and Mech. Engr., Princeton Univ.

Hopkins, J., and Inouye, M. 1971 An Evaluation of Theories for Predicting Turbulent Skin Friction and Heat Transfer on Flat Plates at Supersonic and Hypersonic Mach Numbers AIAA J., Vol. 9, pp. 993-1003.

Horstman, C. 1984a A Computational Study of Complex Three-Dimensional Compressible Turbulent Flow Fields. AIAA Paper No. 84-1556.

Horstman, C. 1984b Private Communications : June 1984, July 1984, October 1984, November 1984.

Jones, W., and Launder, B. 1972 The Prediction of Laminarization with a Two-Equation Model of Turbulence. Int. J. Heat and Mass Transfer, Vol. 15, pp. 301-304.

Kline, S., Cantwell, B., and Lilley, B. 1981 1980-81 AFOSR-HTTM-Stanford Conference on Complex Turbulent Flows. Thermosciences Div., Mech. Engr. Dept., Stanford Univ.

Knight, D. 1981 Theoretical Investigation of Three-Dimensional Shock Wave-Turbulent Boundary Layer Interactions. Research

Proposal Submitted to the Air Force Office of Scientific Research.

Knight, D. 1982 Theoretical Investigation of Three-Dimensional Shock Wave-Turbulent Boundary Layer Interactions. Interim Report for Period 1 Oct 81 to 30 Sept 82; also Report RU-TR-157-MAE-F.

Knight, D. 1983 Theoretical Investigation of Three-Dimensional Shock Wave-Turbulent Boundary Layer Interactions - Part II. Interim Report for Period 1 Oct 82 to 30 Sept 83; also Report RU-TR-160-MAE-F.

Knight, D. 1984a Numerical Simulation of 3-D Shock Turbulent Boundary Layer Interaction Generated by a Sharp Fin. AIAA Paper No. 84-1559.

Knight, D. 1984b A Hybrid Explicit-Implicit Numerical Algorithm for the Three-Dimensional Compressible Navier-Stokes Equations. AIAA J., Vol. 22, pp. 1056-1063.

Knight, D. 1984c Modelling of Three-Dimensional Shock Wave Turbulent Boundary Layer Interactions. Conf. on Macroscopic Modelling of Turbulent Flows and Fluid Mixtures. INRIA, France. To appear, Springer-Verlag.

Knight, J. 1979 SL/1 Manual. Analysis and Computation Division, Programming Techniques Branch, NASA Langley Research Center (revised October 1981)

Korkegi, R. 1976 On the Structure of Three-Dimensional Shock-Induced Separated Flow Regions. AIAA J., Vol. 14, pp. 597-600.

Kubota, H., and Stollery, J. 1982 An Experimental Study of the Interaction Between a Glancing Shock Wave and a Turbulent Boundary Layer J. Fluid Mech., Vol. 116, pp. 431-458.

MacCormack, R. 1982 A Numerical Method for Solving the Equations of Compressible Viscous Flow. AIAA J., Vol. 20, pp. 1275-1281.

McClure, W. 1983 An Experimental Study into the Scaling of an Unswept Sharp-Fin-Generated Shock/Turbulent Boundary Layer Interaction. M.S.E. Thesis, Dept. Mech. and Aero. Engr., Princeton Univ.

McClure, W.,and Dolling,D. 1983 Flowfield Scaling in Sharp Fin-Induced Shock Wave Turbulent Boundary Layer Interaction. AIAA Paper No. 83-1754.

McKenzie, T. 1983 A Flow Field Scaling of the Three-Dimensional Shock/Boundary Layer Interaction of the Swept Compression Corner. MSE Thesis, Dept. of Mech. and Aero. Engr., Princeton Univ.

Oskam, B., Vas, I., and Bogdonoff, S. 1976 Mach 3 Oblique Shock Wave/Turbulent Boundary Layer Interactions in Three Dimensions. AIAA Paper No. 76-336.

Oskam, B., Vas, I., and Bogdonoff, S. 1977 An Experimental Study of Three-Dimensional Flow Fields in an Axial Corner at Mach 3. AIAA Paper No. 77-689.

Schubauer, G., and Klebanoff, P. 1950 Investigation of Separation of the Turbulent Boundary Layer. NACA Technical Note No. 2133.

Settles, G., Perkins, J., and Bogdonoff, S. 1980 Investigation of Three-Dimensional Shock/Boundary Layer Interaction at Swept Compression Corners. AIAA J., Vol. 18, pp. 779-785.

Settles, G., and Bogdonoff, S. 1982 Scaling of Two- and Three-Dimensional Shock/Turbulent Boundary Layer Interactions at Compression Corners. AIAA J., Vol. 20, pp. 782-789.

Settles, G., Horstman, C., and McKenzie, T. 1984 Flowfield Scaling of a Swept Compression Corner Interaction - A Comparison of Experiment and Computation. AIAA Paper No. 84-0096.

Settles, G., and Teng, H. 1984 Cylindrical and Conical Upstream Influence Regions of Three-Dimensional Shock/Turbulent Boundary Layer Interactions. AIAA J., Vol. 22, pp. 194-200.

Token, K. 1974 Heat Transfer Due to Shock Wave/Turbulent Boundary Layer Interactions on High Speed Weapons Systems. AFFDL-TR-74-77.

Viegas, J. and Rubesin, M. 1983 Wall-Function Boundary Conditions in the Solution of the Navier-Stokes Equations for Complex Compressible Flows. AIAA Paper No. 83-1694.

Visbal, M. 1983 Numerical Simulation of Shock/Turbulent Boundary Layer Interactions Over 2-D Compression Corners. Ph.D. Thesis, Dept. of Mech. and Aero. Engr., Rutgers Univ.

Visbal, M., and Knight, D. 1984 The Baldwin-Lomax Turbulence Model for Two-Dimensional Shock-Wave/Boundary Layer Interactions. AIAA J., Vol. 22, pp. 921-928.

York, B. 1984 Evaluation of the Baldwin-Lomax Turbulence Model for a Class of Boundary Layer Flows. M. S. Thesis, Dept. Mech. and Aero. Engr., Rutgers Univ.

York, B., and Knight, D. 1985 Calculation of a Class of Two-Dimensional Turbulent Boundary Layer Flows using the Baldwin-Lomax Model. AIAA Paper No. 85-0126.

Zheltovodov, A. 1982 Regimes and Properties of 3-D Separation

Flows Initiated by Skewed Compression Shocks. Zhurnal Prikladnoi Mekhaniki i Teknicheskoi Fiziki, No. 3, pp. 116-123.

Zwarts, F. 1970 The Compressible Turbulent Boundary Layer in a Pressure Gradient. Ph.D. Thesis, McGill U.

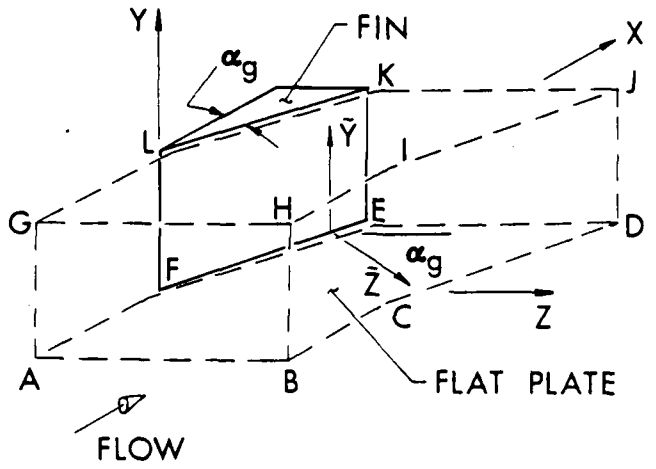

Fig. 1 Physical Region for 3-D Sharp Fin

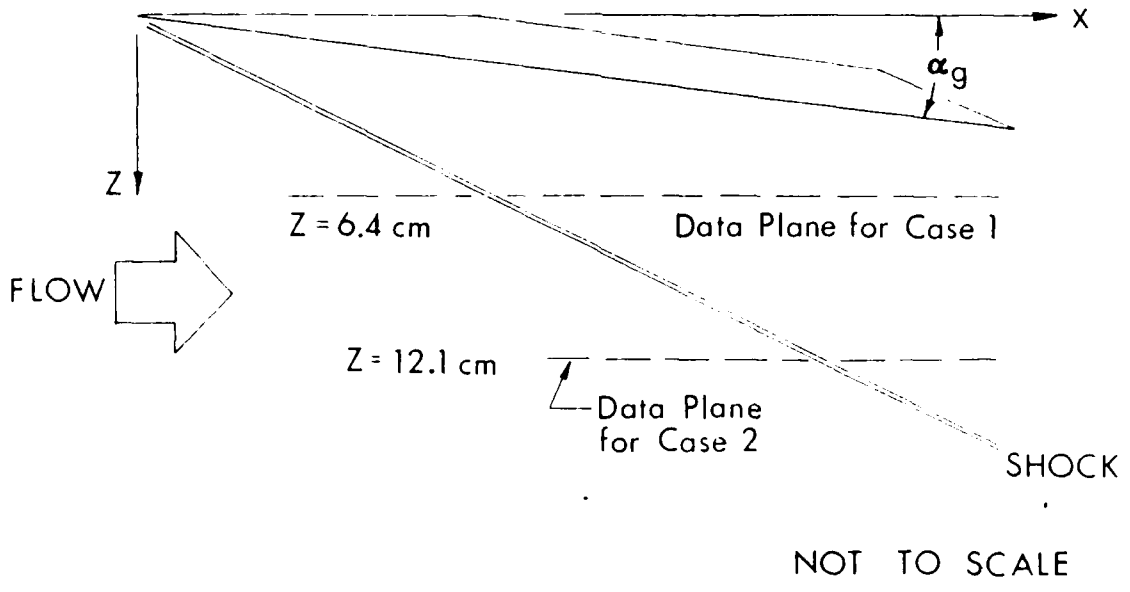

Fig. 2 Experimental Data Stations of McClure and Dolling

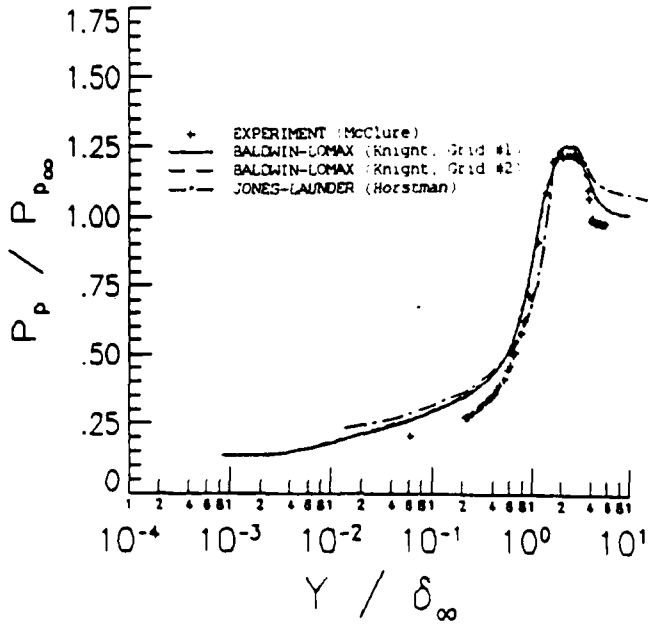

Fig. 3a Pitot Pressure at $x_s = -1.7\delta_o$ for $\alpha_g = 10$ deg (Case 1)

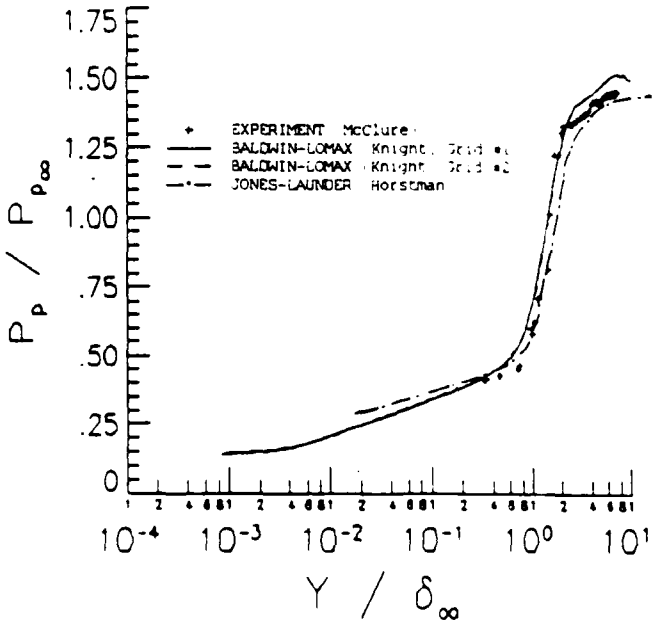

Fig. 3b Pitot Pressure at $x_s = 1.0\delta_o$ for $\alpha_g = 10$ deg (Case 1)

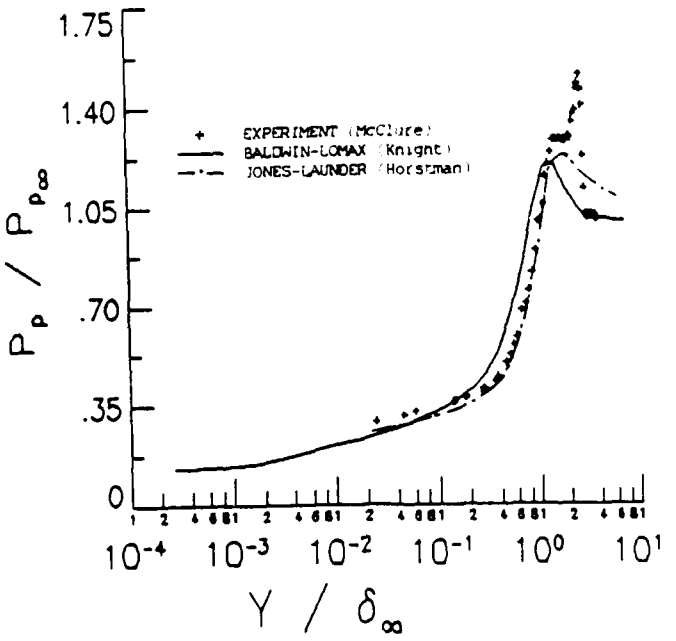

Fig. 4a Pitot Pressure at $x_s = -1.47\delta_o$ for $\alpha_g = 10$ deg (Case 2)

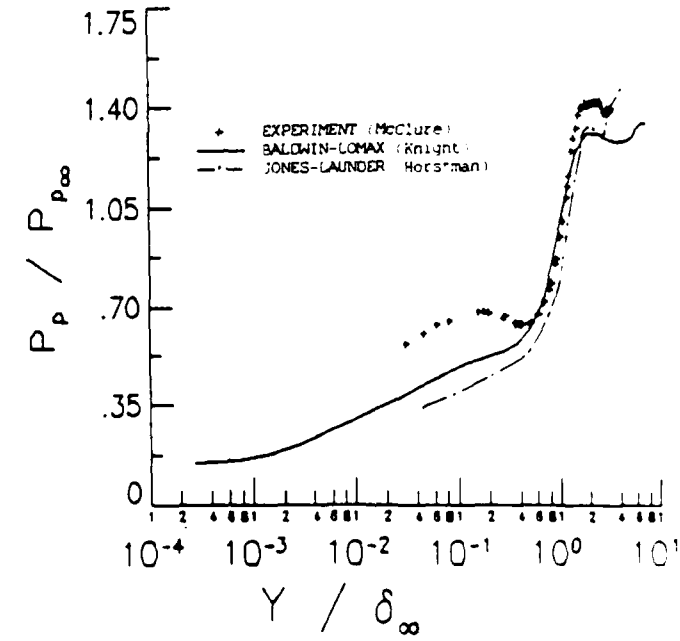

Fig. 4b Pitot Pressure at $x_s = 3.46\delta_o$ for $\alpha_g = 10$ deg (Case 2)

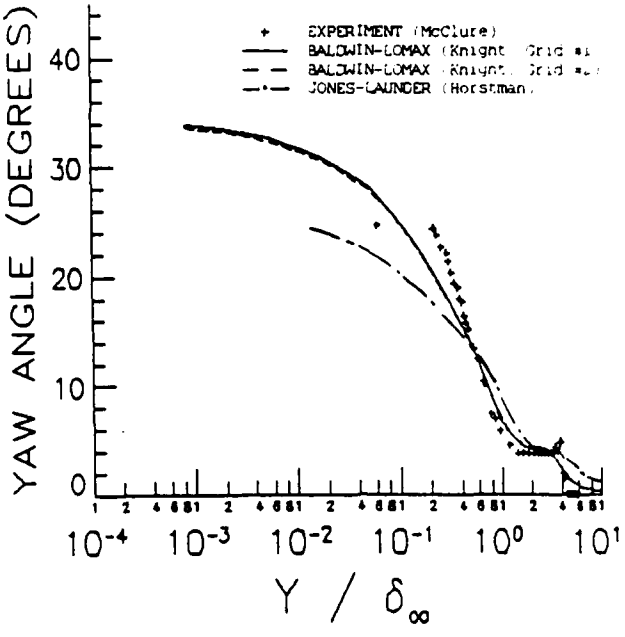

Fig. 5a Yaw Angle at $x_s = -1.7\delta_0$ for $\alpha_g = 10$ deg (Case 1)

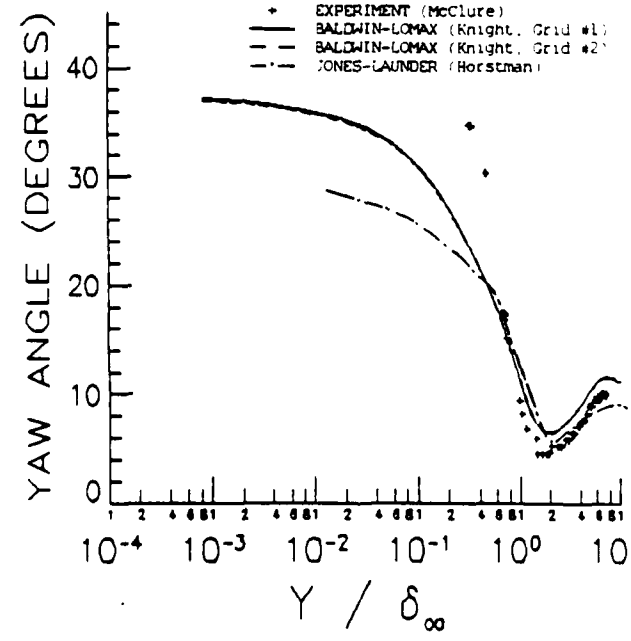

Fig. 5b Yaw Angle at $x_s = 1.0\delta_0$ for $\alpha_g = 10$ deg (Case 1)

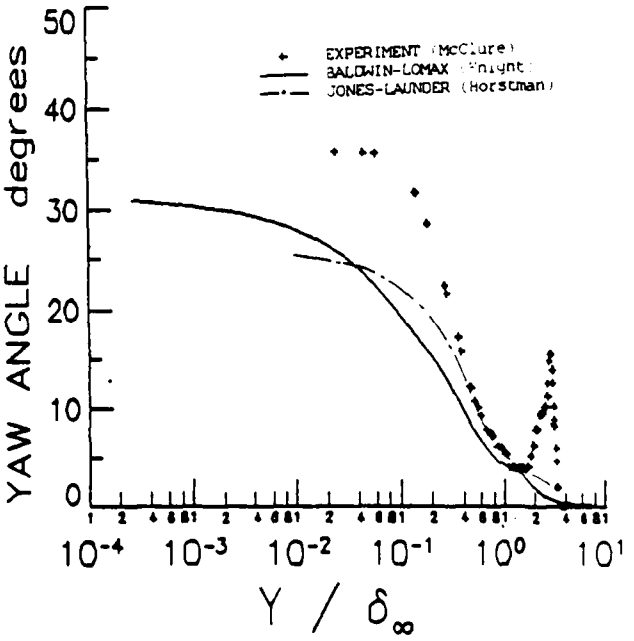

Fig. 6a Yaw Angle at $x_s = -1.47\delta_o$ for $\alpha_g = 10$ deg (Case 2)

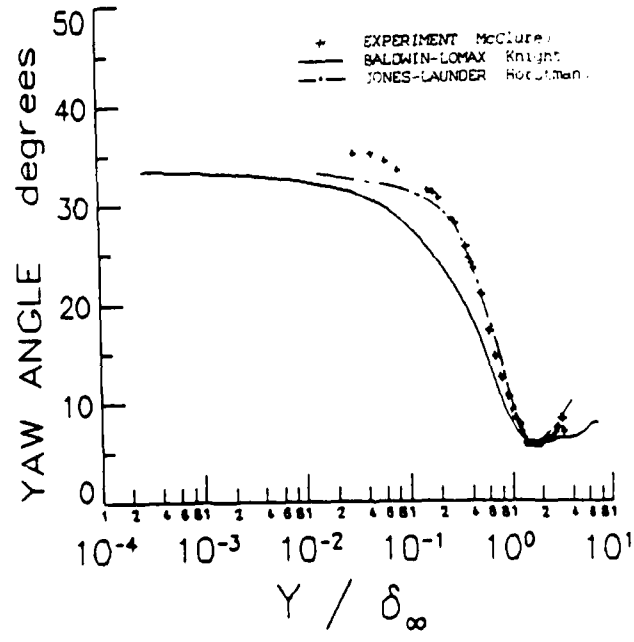

Fig. 6b Yaw Angle at $x_s = 3.40\delta_o$ for $\alpha_g = 10$ deg (Case 2)

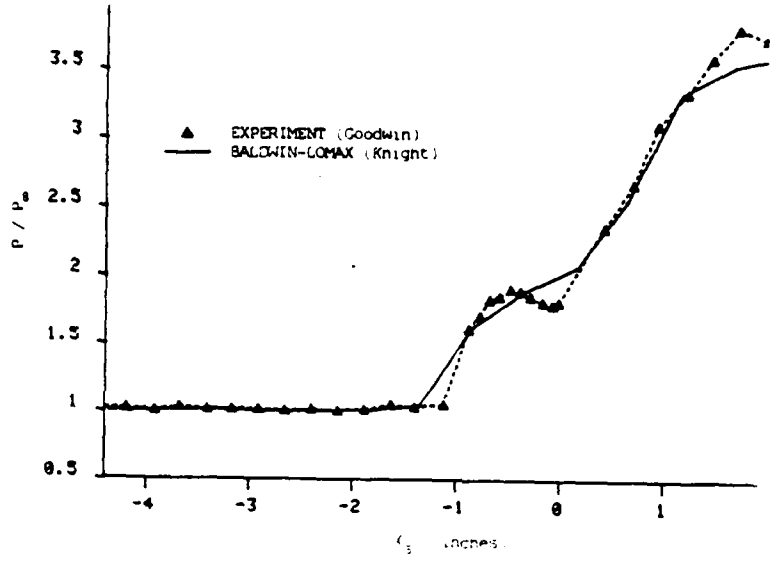

Fig. 7a Surface Pressure at z=3.71 cm for α_g = 2Ø deg

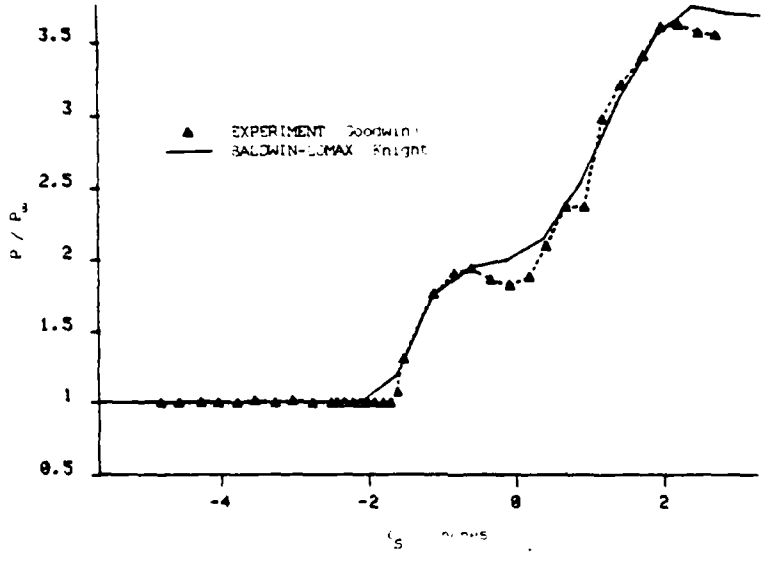

Fig. 7b Surface Pressure at z=6.25 cm for α_g = 2Ø deg

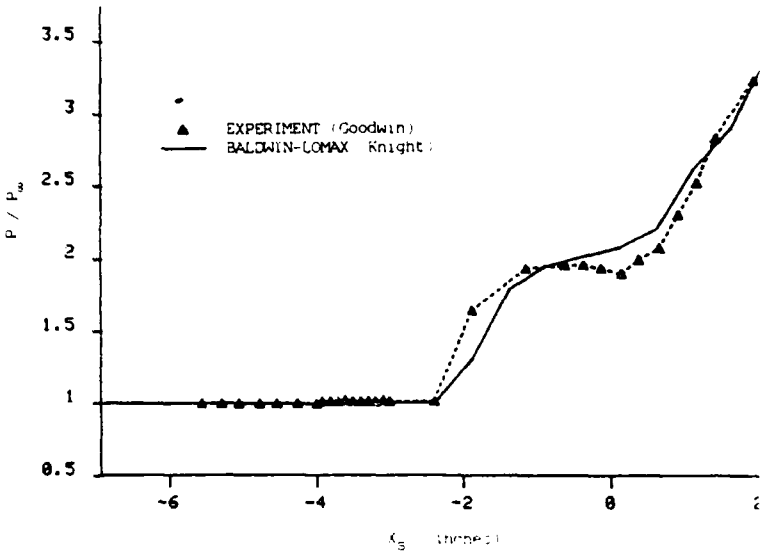

Fig. 7c Surface Pressure at z=8.79 cm for α_g = 2Ø deg

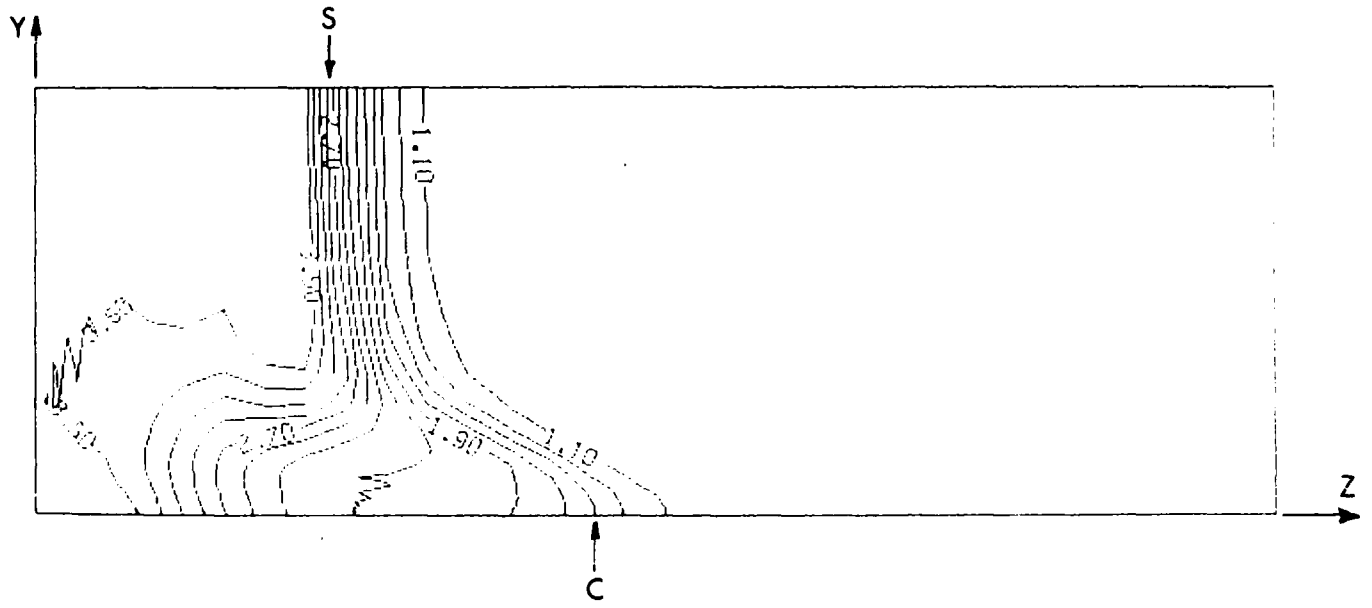

Fig. 8 Static Pressure contours at x = $13\delta_\infty$ for α_g = 2Ø deg

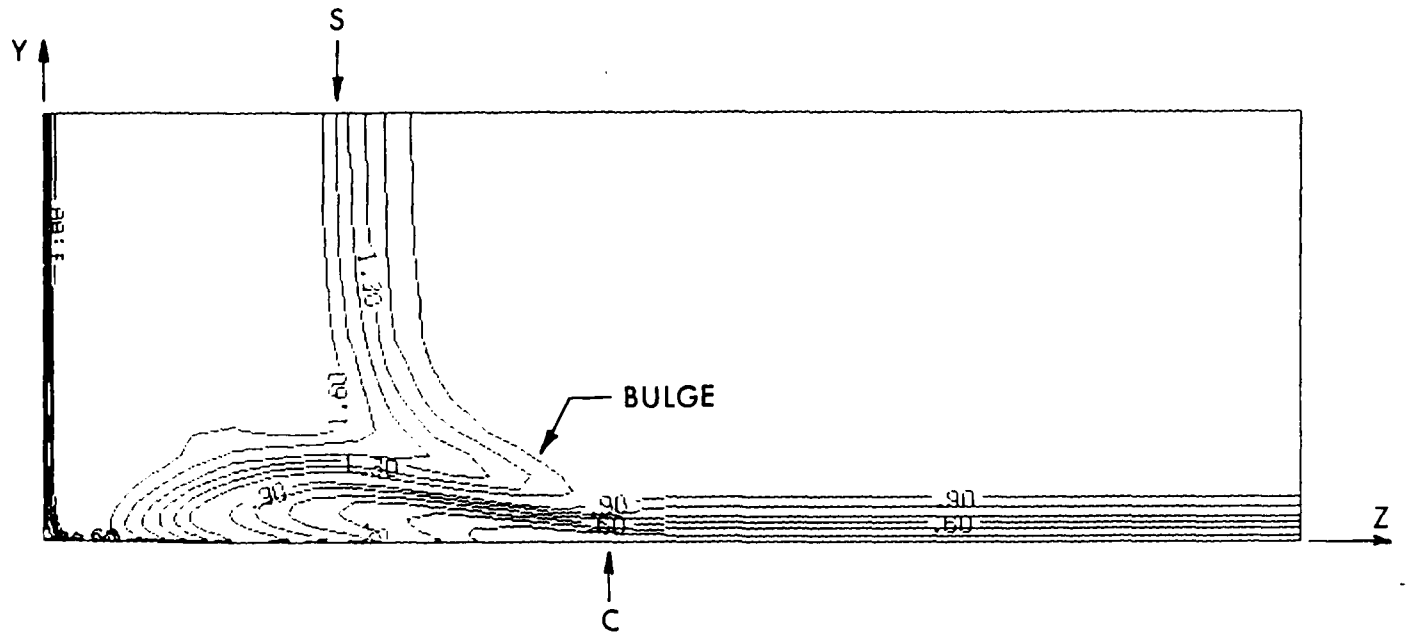

Fig. 9 Pitot Pressure contours at $x = 13\delta_\infty$ for $\alpha_g = 20$ deg

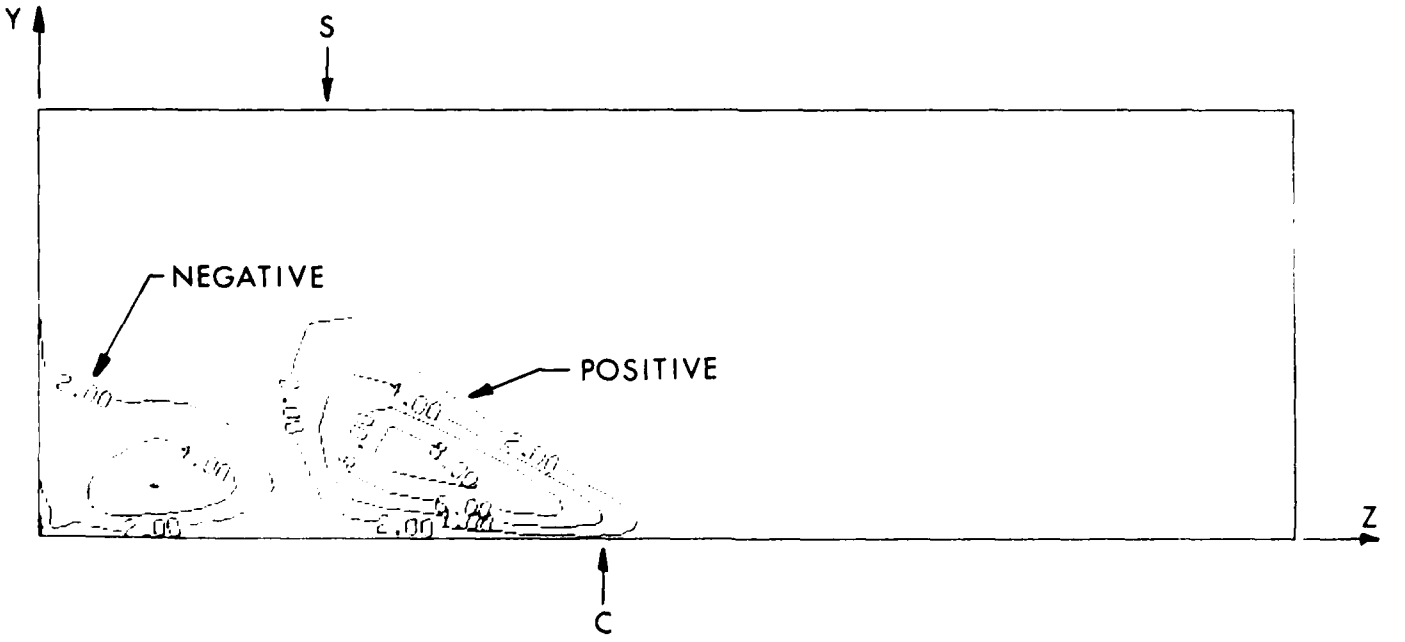

Fig. 10 Pitch Angle contours at $x = 13\delta_\infty$ for $\alpha_g = 20$ deg

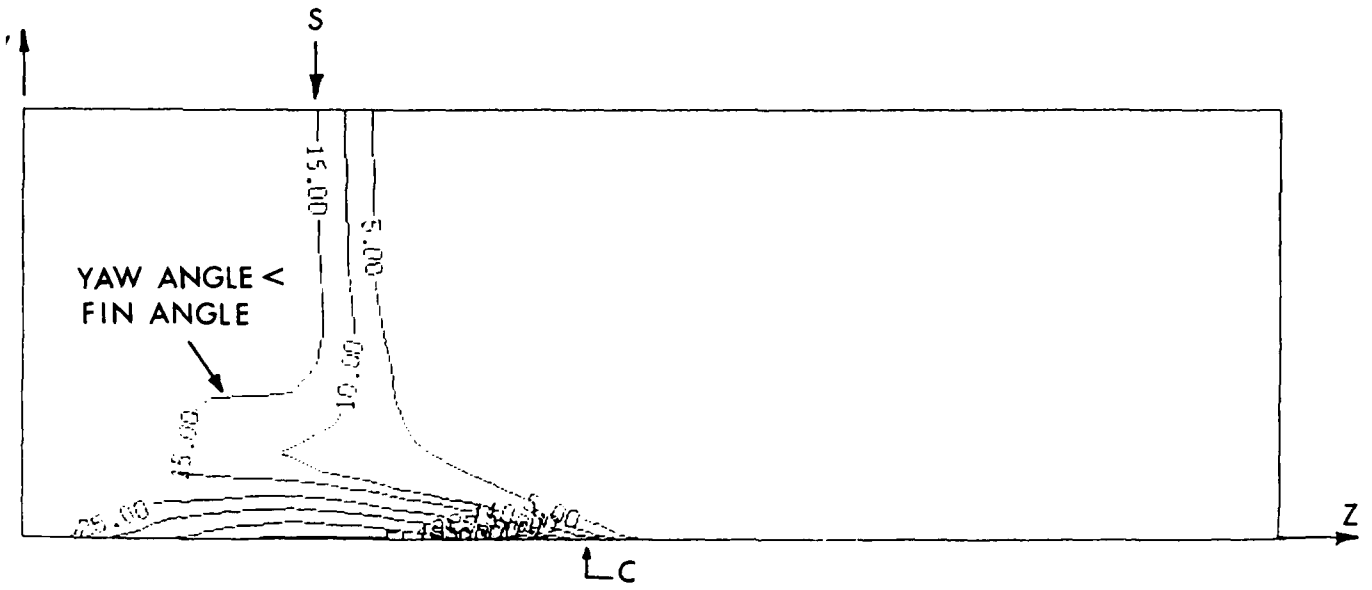

Fig. 11 Yaw Angle contours at $x = 13\delta_\infty$ for $\alpha_g = 20$ deg

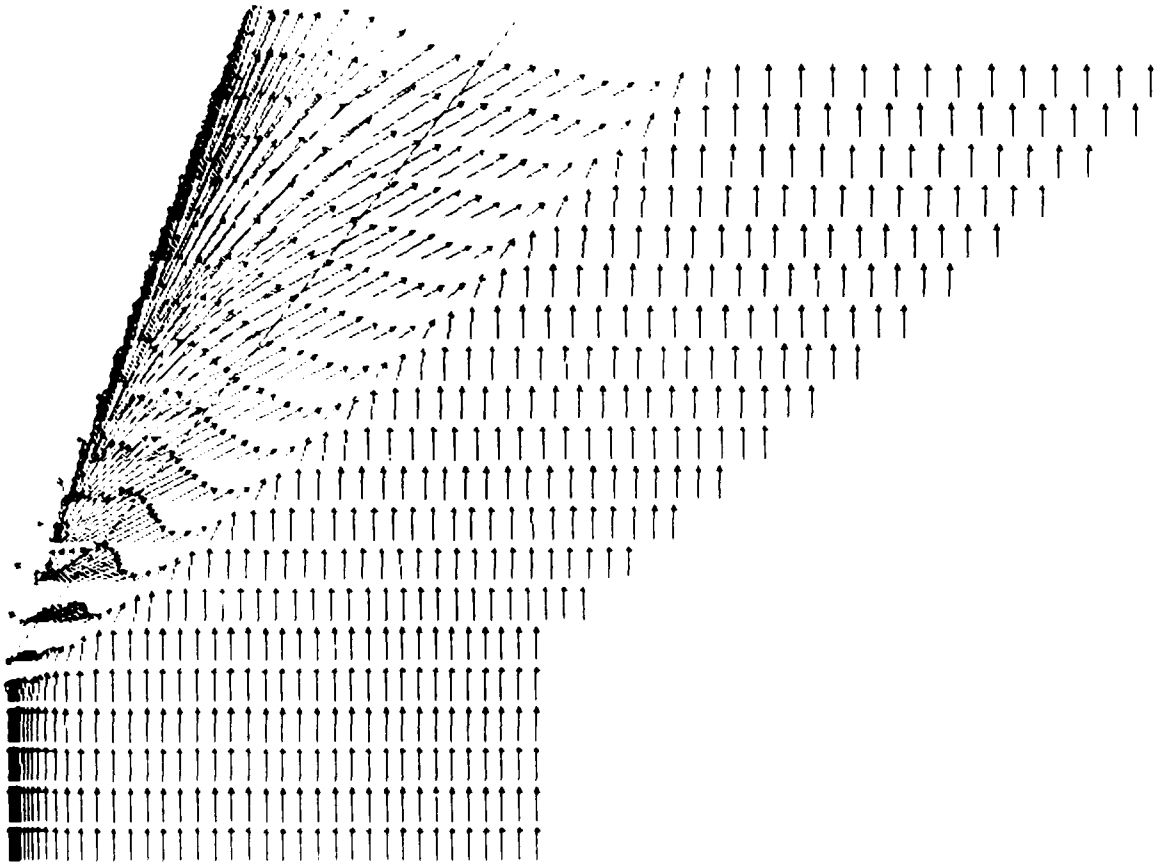

Fig. 12 Surface Streamlines on Flat Plate for $\alpha_g = 20$ deg

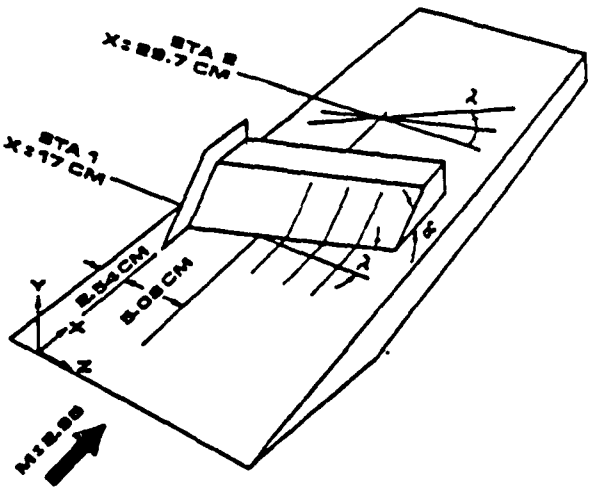

Fig. 13 3-D Swept Compression Corner

END

FILMED

5-85

DTIC